p. 832 The Amors, Apollos, & Atens have orbits between Earth & Mars, crossing Earth's orbit near perihelion, or near aphelion respectively.

p. 833 Hirayama Families
>100 families of asteroids w/ nearly identical orbits.
Each family was probably originally of larger asteroid which suffered a collision.

p. 833 Rendezvousing w/ Asteroids
The Galileo spacecraft on its way to Jupiter flew by 951 Gaspra in 1991 & 243 Ida in 1993 (Ida + moon Dactyl are shown in Fig. 22.12)

Kepler's 3rd Law of Dactyl orbiting Ida ⇒ Ida mass = $3-4\times10^{16}$ kg, ρ = 2200-2900 $\frac{kg}{m^3}$
Near Earth Asteroid Rendezvous (NEAR-Shoemaker) launched in 1996.
Went into orbit around 433 Eros on 2/14/2000 (Valentine's Day? Really?)
(Fig. 22.16) 33×8 km. Not designed as lander, but >1 yr in orbit descended & landed at 1.6 $\frac{m}{s}$ (Fig. 22.17)
After it landed it measured γ-ray spectrum, found elements. (Fig. 22.18)

p. 835 Classes of Asteroids
Different colors, different compositions (Fig. 22.19)

p. 837 Internal Heating
There is evidence that the interiors of some asteroids were molten in the past.
People have made models involving radioactive decay, but the models have some problems.

Ch. 24 The Milky Way Galaxy

§24.1 Counting the Stars in the Sky

It's difficult to observe our Milky Way galaxy, due to dust & gas.

p. 875 Historical Models of the Milky Way Galaxy (Fig. 24.1)
In dark skies, anyone can see band of light, inclined ~60° w/rt equator.
Galileo, w/ his telescope, saw that it is a huge collection of stars.
William Herschel (1738-1804) made map (Fig 24.2) assuming (1) all stars have ~same intrinsic magnitude (2) number density in space ~constant (3) no obscuration (4) he could see to edges of distribution.
Concluded that Sun near center.
Jacobus Kapteyn (1851-1922) model (Fig 24.3) used more quantitative methods, but also came up w/ distance estimates. Sun is actually ~8 kpc from galactic center.
1915-1919 Harlow Shapley estimated distances to globular clusters.

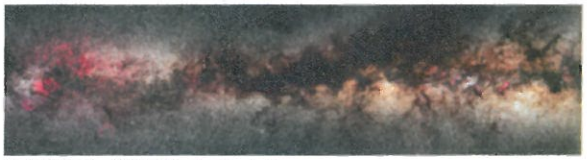

Fig. 24.1 Mosaic of Milky Way showing dust lanes.

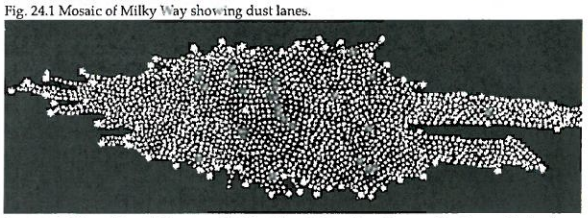

Fig. 24.2 William Herschel's map of Milky Way Galaxy, based on qualitative analysis of star counts. He believed that Sun (larger star) resided near center.

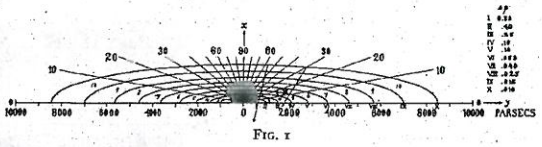

Fig. 24.3 The Kapteyn (1922) universe. Surfaces of constant stellar number density are indicated around the Galactic center.

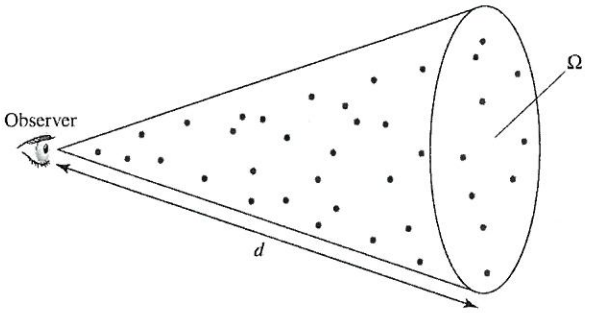

Fig. 24.4 Observer on Earth counting number of stars within specified range of spectral & luminosity types out to distance d within cone of solid angle Ω.

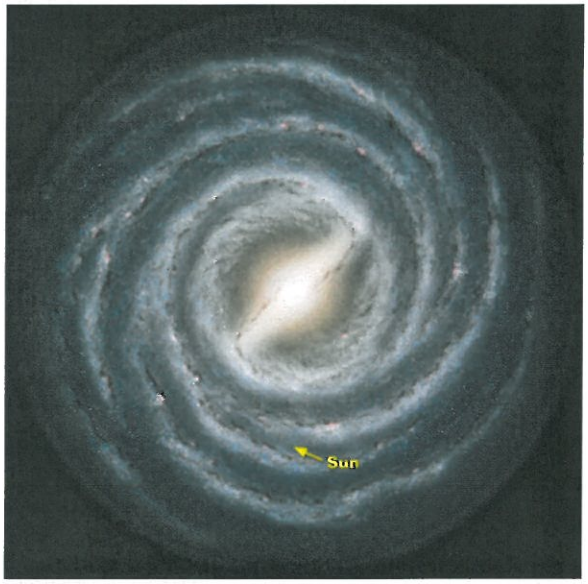

Fig. 24.5 Artist's conception of Milky Way Galaxy seen face-on.

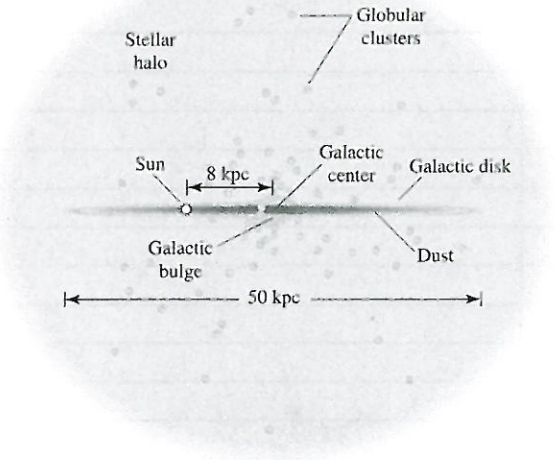

Fig. 24.6 Edge-on diagram of the Galaxy, not strictly to scale; see Table 24.1.

this estimate of diameter of MW was ~100 kpc, ~10× Kapteyn's.
(actual diameter ~30 kpc)

p. 878 the Effects of Interstellar Extinction

From eq. 12.1, $d = 10^{(m_\lambda - M_\lambda - A_\lambda + 5)/5} = d' 10^{-A_\lambda/5}$

where $d' = 10^{(m_\lambda - M_\lambda + 5)/5}$ is erroneous distance estimate from neglecting extinction, & A_λ is extinction in magnitudes.

In Milky Way, visible extinction ~ 1 magnitude / kpc

$A > 0$, so $d < d'$: true distance < estimate

Ex. 24.1 p. 878 B0 ms * w $M_V = -4.0$, apparent visual magnitude $V = +8.2$. $d' = 10^{(-M_V+5)/5} = 2800$ pc

Suppose reddening ⇒ extinction = 1 mag kpc^{-1} ⇒ $A_V = kd$, $k = 10^{-3}$ mag pc^{-1} (d in pc)

$d = 10^{(V - M_V - kd + 5)/5} = 2800 \times 10^{-kd/5}$ pc

Solve numerically ⇒ $d = 1400$ pc

p. 878 Differential & Integrated Star Counts - skip

Modern star count uses automated CCD detectors.

But there are still significant uncertainties in stellar distributions.

§24.2 The Morphology of the Galaxy p. 881

There are still significant uncertainties, but here's the basic picture.

p. 882 Distance to the Galactic Center (GC)

(Fig. 24.5 + 24.6)

Solar Galactocentric distance $R_0 \sim 8$ kpc ~ 1/3 of Galactic radius.

p. 883 The Structure of the Thin & Thick Disks

Disk has 2 major components. (Table 24.1, top)

Thin disk: relatively young stars, dust gas, vertical scale height $z_{thin} \sim 350$ pc

Thick disk: older stars, $z_{thick} \sim 1000$ pc

$$n(z, R) = n_0 \left(e^{-z/z_{thin}} + 0.085\, e^{-z/z_{thick}} \right) e^{-R/h_R}$$

R = cylindrical radius, $h_R > 2.25$ kpc, $n_0 \sim 0.02$ stars pc^{-3}

p. 885 The Age-Metallicity Relation

From §13.3 populations of stars: mass fraction of "metals"

Population I - metal-rich $Z \sim 0.02$ (youngest), Population II - metal-poor $Z \sim 0.001$, Population III $Z \sim 0$ (oldest, if those still exist).

metallicity defined by $[Fe/H] = \log_{10} \left[\frac{(N_{Fe}/N_H)_{star}}{(N_{Fe}/N_H)_\odot} \right]$

Disks			
	Neutral Gas	Thin Disk	Thick Disk
M (10^{10} $M_\odot$)	0.5[a]	6	0.2 to 0.4
L_B (10^{10} $L_\odot$)[b]	—	1.8	0.02
M/L_B ($M_\odot/L_\odot$)	—	3	—
Radius (kpc)	25	25	25
Form	e^{-z/h_z}	e^{-z/h_z}	e^{-z/h_z}
Scale height (kpc)	< 0.1	0.35	1
σ_w (km s^{-1})	5	16	35
[Fe/H]	> +0.1	−0.5 to +0.3	−2.2 to −0.5
Age (Gyr)	$\lesssim$ 10	8[c]	10[d]

Spheroids			
	Central Bulge[e]	Stellar Halo	Dark-Matter Halo
M (10^{10} $M_\odot$)	1	0.3	190^{+360}_{-170}[f]
L_B (10^{10} $L_\odot$)[b]	0.3	0.1	0
M/L_B ($M_\odot/L_\odot$)	3	~ 1	—
Radius (kpc)	4	> 100	> 230
Form	boxy with bar	$r^{-3.5}$	$(r/a)^{-1}\,(1+r/a)^{-2}$
Scale height (kpc)	0.1 to 0.5[g]	3	170
σ_w (km s^{-1})	55 to 130[h]	95	—
[Fe/H]	−2 to 0.5	< −5.4 to −0.5	—
Age (Gyr)	< 0.2 to 10	11 to 13	~ 13.5

[a] $M_{\rm thin}/M_{\rm gas} \simeq 0.007$.

[b] The total luminosity of the Galaxy is $L_{B,\rm tot} = 2.3 \pm 0.6 \times 10^{10}\ L_\odot$, $L_{\rm bol,tot} = 3.6 \times 10^{10}\ L_\odot$ (~ 30% in IR).

[c] Some open clusters associated with the thin disk may exceed 10 Gyr.

[d] Major star formation in the thick disk may have occurred 7–8 Gyr ago.

[e] The mass of the black hole in Sgr A* is $M_{\rm bh} = 3.7 \pm 0.2 \times 10^6\ M_\odot$.

[f] $M = 5.4^{+6.2}_{-3.6} \times 10^{11}\ M_\odot$ within 50 kpc of the center.

[g] Bulge scale heights depend on age of stars: 100 pc for young stars, 500 pc for old stars.

[h] Dispersions increase from 55 km s^{-1} at 5 pc to 130 km s^{-1} at 200 pc.

Table 24.1 Approximate values for various parameters associated with components of the Milky Way Galaxy.

Fig. 24.7 Andromeda Galaxy = M31 = NGC 224, spiral galaxy believed to be much like Milky Way, 770 kpc away.

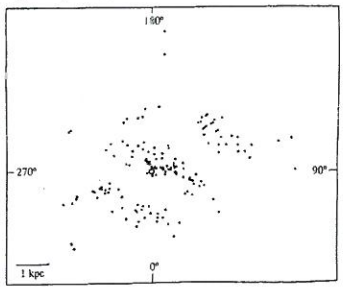

Fig. 24.8 Spatial distribution of young Galactic clusters & H II regions reveals presence of spiral arms within disk of Galaxy.

Fig. 24.9 NGC 891 seen edge-on, clearly shows thin dust band in plane of disk. Milky Way probably appears very similar.

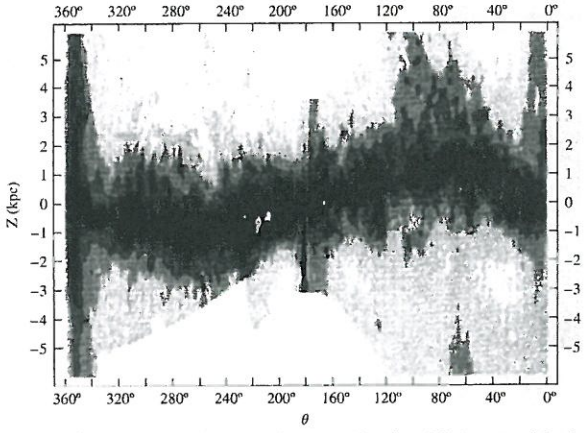

Fig. 24.10 The H I warp in Milky Way at distance 13.6 kpc from Galactic center. Galaxy's midplane is at z = 0, & direction toward center of Milky Way is at 0°.

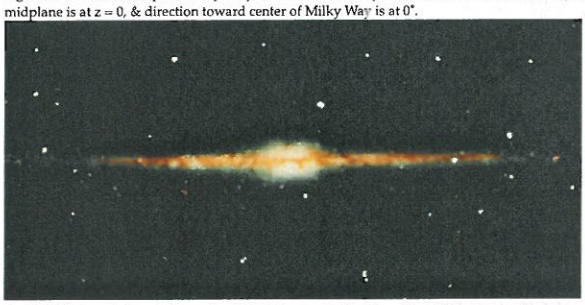

Fig. 24.11 Infrared view of Galaxy by COBE. It extends 96° either side of Galactic center.

As time goes on, interstellar medium ISM enriched by SNe, so younger star should have higher metallicity, but there are many complicating factors, so the relationship is unreliable.

p. 886 Age Estimates of the Thin + Thick Disks

Thin disk: $-0.5 < [Fe/H] < 0.3$, star formation started ~ 8 Gyr ago + continues today.

thick disk $-0.6 < [Fe/H] < -0.4$, stars formed 10-11 Gyr ago.

Mass-to-Light Ratios

Thin disk $M/L_B = 6.5\times10^{10} M_\odot / 1.8\times10^{10} L_\odot \approx 3 M_\odot/L_\odot \Rightarrow \langle M \rangle = 0.7 M_\odot$ ← lower mass, long lived stars

L_B = blue luminosity

thick disk $M/L_B = (2-4)\times10^9 M_\odot / 3\times10^8 L_\odot \approx 10-20 M_\odot/L_\odot$

p 887 Spiral Structure

Disk contains spiral structure (Fig 24.7 Andromeda)

Spiral arms are active star-formation regions.

Sun is close to, but not in Orion arm (Fig. 24.8)

Dust + gas are predominantly in midplane + spiral arms (Fig. 24.9 NGC 891)

p. 889 Interstellar Gas + Dust

Stars are formed from gas + dust clouds,

Mapped by obscuration + 21-cm HI emission.

$M_{HI} \sim 4\times10^9 M_\odot$, $M_{H_2} \sim 10^9 M_\odot$

HI in outer part of galaxy is not just in plane, but shows warp up to 15° from plane (Fig. 24.10)

ABB there is $\sim 10^9 M_\odot$ of hot tenuous gas, ~spherical w/ R ~ 70 kpc.

p. 891 The Disruption of Satellite Galaxies

Magellanic Stream = narrow band of HI stretching 180° across sky = result of tidal interaction w/ LMC (52 kpc away) + SMC (61 kpc) 200 Myr ago.

There is a dwarf spheroidal galaxy 16 kpc from GC, being incorporated into Galaxy.

Other unusual globular clusters are probably also dwarfs,

when galaxies collide, stars pass through but clouds stop.

p 891 The Galactic Bulge

the GB has a scale height up to 500 pc, only slightly larger than thin disk, but seems to be independent component. (Fig 24.11)

p 893 the Milky Way's Central Bar (Fig 24.5)

Bar radius ($\frac{1}{2}$ length) 4.4 ± 0.5 kpc

p. 893 the 3-kpc Expanding Arm
Gas cloud moving towards us at 50 km s^{-1},
Probably in elliptical orbit around GC driven by gravitational perturbations from bar,
p 894 the Stellar Halo & Globular Cluster System
(Stellar) halo = globular clusters & field stars (not in gc's) w/ large velocities ⊥ to plane.
2 populations (Fig. 24.12)
older - metal-poor clusters in extended halo
younger, higher metallicity clusters in much flatter distribution,
Galaxy has ~150 clusters, ranging from 11-13 Gyr old.
Sum of all luminous components: $L_{B,tot} \sim 2.3 \times 10^{10} L_\odot$, $L_{bol} \sim 3.6 \times 10^{10} L_\odot$
p 896 the Dark Matter Halo
$M_{tot,luminous} = 9 \times 10^{10} M_\odot$
But gravitational influences at larger R ⇒ dark matter halo, roughly spherical, extending out to ~230 kpc,
$\rho(r) = \frac{\rho_0}{(r/a)(1+r/a)^2}$. Total mass at <230 kpc = $1.9 \times 10^{12} M_\odot$
~95% of total mass of Galaxy.
Composition:
WIMPs - weakly interacting massive particles, perhaps massive ν's (probably not enough) or neutralinos (supersymmetric partners).
MACHOs - massive compact halo objects - WDs, NSs, BHs, red or brown dwarfs,
Search for MACHOs uses them as grav. lenses (Fig 24.14) (24.15)
But there don't seem to be enough MACHOs to account for dark matter.
p. 897 the Galactic Magnetic Field
~0.4 nT in spiral arms, ~1 μT in Galactic center,
< $B_\oplus$ = 50 μT but may be dynamically important (energy density ~ thermal energy density of gas).
§24.3 The Kinematics of the Milky Way - skip

§24.4 the Galactic Center p. 922
Gas & dust in Galactic plane ⇒ $A_{visible}$ > 30 magnitudes of extinction.
We are 30 pc above plane & 8 kpc from GC, but due to our 7.7 km s^{-1} velocity ⊥ to plane, in 15×10^6 yr we will be able to see it well.

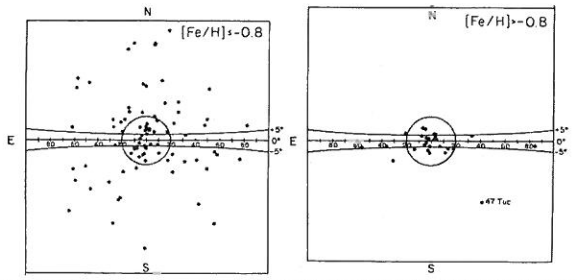

Fig. 24.12 Metal-poor globular clusters form a nearly spherical distribution about the Galactic center, while more metal-rich clusters are found predominantly near the plane of the Galaxy; possibly associated with thick disk (Zinn 1985).

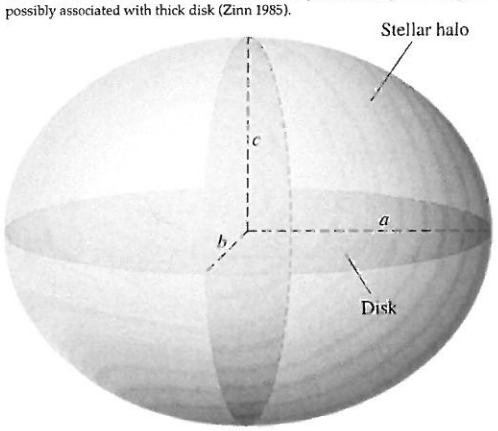

Fig. 24.13 General shape of triaxial spheroidal system with a ≥ b ≥ c. Galactic disk (foreshortened by perspective) is roughly circular.

Fig. 24.14 Gravitational lensing (focusing) of starlight produced by intervening MACHO.

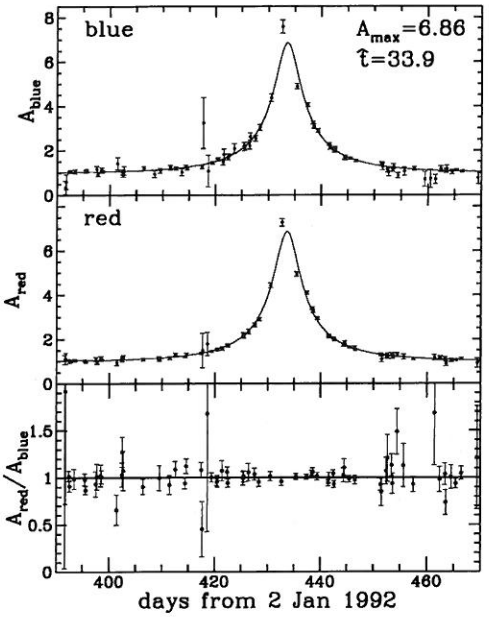

Fig. 24.15 Light curve of a star in LMC brightened over period of 33 days, apparently due to MACHO passing through line of sight.

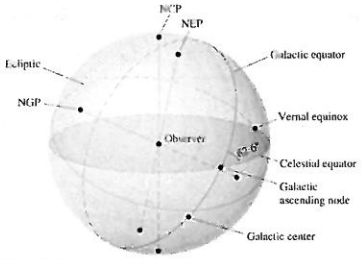

Fig. 24.16

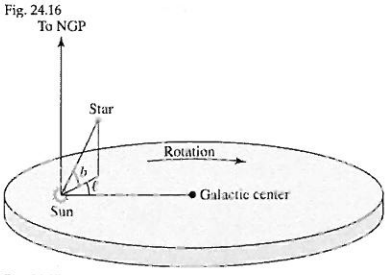

Fig. 24.17

Fig. 24.18

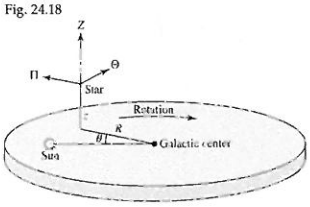

Fig. 24.19

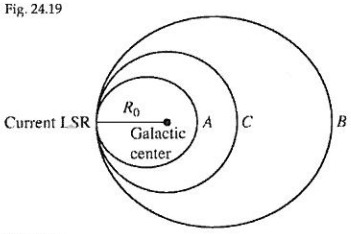

Fig. 24.20

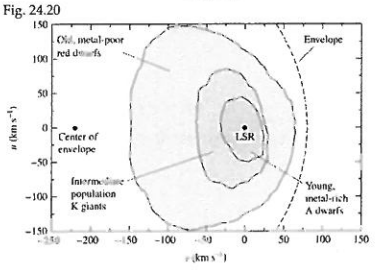

Fig. 24.21

p. 923 - The Mass Distribution Near the Galactic Center

We can observe galactic nucleus in I.R, radio, X + γ-rays.
High density of stars ⇒ close encounters often (every 10^6 yr) ⇒ "isothermal" (Maxwellian) velocity distribution down to r ~ 0.1–1.0 pc.
At smaller r, kepler's 3rd ⇒ higher mass density
Orbits of some stars very close to GC have been followed. Star S2 has P = 15.2 yr, e = 0.87, perigalactic or distance 120 AU. (Fig 24.32)

Ex. 24.4.1 p. 924 Semimajor axis is (Eq. 2.5) $a_{S_2} = r_p(1-e) = 1.4 \times 10^{14}$ m
Kepler's 3rd ⇒ mass interior to orbit = $M = 4\pi^2 a_{S_2}^3 / GP^2 = 3.5 \times 10^6 M_\odot$
More precise calculation ⇒ $M = 3.7 \pm 0.2 \times 10^6 M_\odot$ (Fig. 24.33)

p. 926 Radio Sources in Sagittarius

The VLA has an angular resolution ≤ 0.1". At 8000 pc, this is a distance 800 AU.
So we can see details of this active regions. (Actually better than this)
(Fig. 24.34) Filaments may be mass outflow from GC. Sgr A is the radio source,
there is a molecular circumnuclear ring, torous w/ inner + outer radii 2 pc + 8 pc, much denser + hotter than typical molecular clouds.
Ring shows evidence of recent energetic activity, maybe SN in last 10^5 yrs.
In fact Sgr A East is a SN remnant 100–5000 yrs old.
Sgr A West is an unusual HII region containing the strong unresolved radio source Sgr A* (Fig. 24.35)
Sgr A* is also very near the brightness peak of the central stellar cluster,
Sgr A* is probably the actual center of the Galaxy.

Ex. 24.4.2 p. 929 Gas cloud 0.3 pc from GC w/ V = 260 km s^{-1} ⇒
$M_r = \frac{V^2 r}{G} = 4.7 \times 10^6 M_\odot$

An X-ray Source in Sgr A

Uncertain due to absorption, but T ~ 10^8 K, L (soft X-rays) ~ 10^{28} W,
L (hard X-rays) ~ 2×10^{31} W
Highly variable ⇒ size ≤ 0.1 pc (light travel time)

The Supermassive BH in Sgr A*

By following orbits of individual stars ⇒ R < 2 AU ⇒ supermassive BH
w/ $M = 3.7 \pm 0.2 \times 10^6 M_\odot$ ⇒ $R_S = 0.08$ AU $= 16 R_\odot$
Observing density + velocities of matter near GC ⇒ $\dot{M} = 10^{-3} - 10^{-2} M_\odot$ yr^{-1}.
Virial theorem ⇒ L = ½ rate of change of potential energy,
With $r_f = R_S$ + $r_i >> R_S$ this is $L = \frac{1}{2} \frac{G M_{bh} \dot{M}}{R_S} = \frac{1}{4} \dot{M} c^2$
Need L ~ $10^7 L_\odot$ for degree of ionization observed ⇒
$\dot{M} = \frac{4L}{c^2} = 2.7 \times 10^{-6} M_\odot$ yr^{-1} (so there's plenty of energy available).
Sgr A* has X-ray flares (160 × quiescent) ~ 1/day.

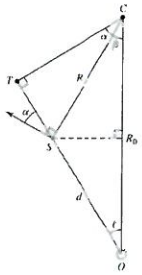

Fig. 24.22

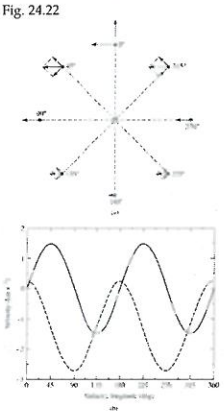

Fig. 24.23

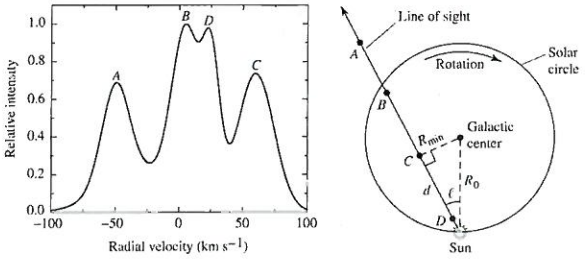

Fig. 24.24

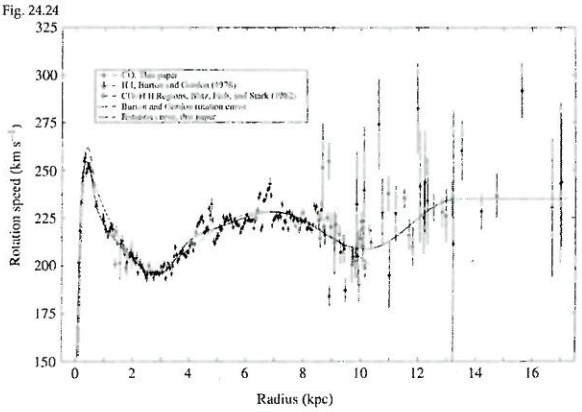

Fig. 24.25

Fig. 24.26

Fig. 24.27

Fig. 24.28

Fig. 24.29

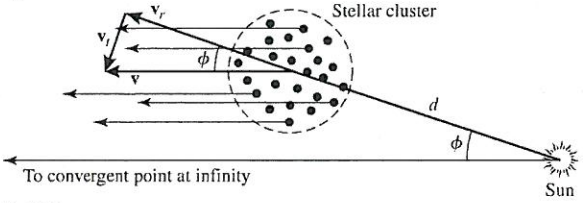

Fig. 24.30

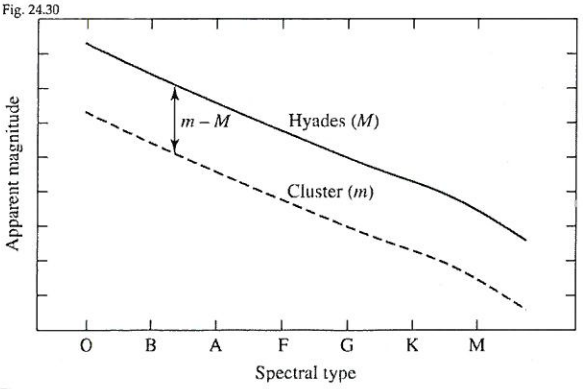

Fig. 24.31

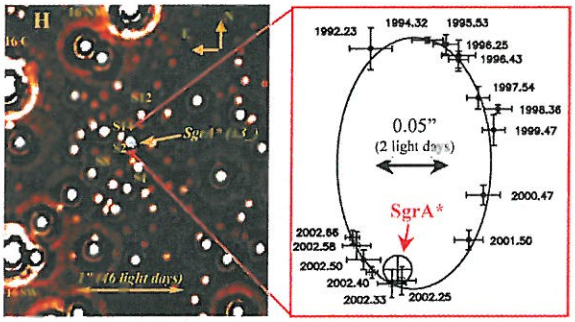

Fig. 24.32 The orbit of S2 about the center of the Milky Way. The center is designated as Sgr A*.

49c

3/10/16

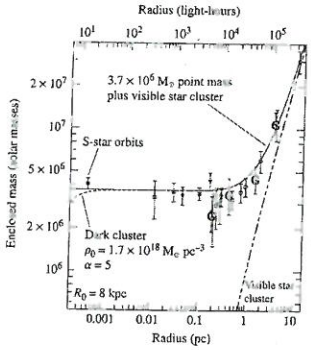

FIGURE 24.33 The interior mass function for the central 10 pc of the Galaxy. Note that the curve is consistent with a mass distribution $M_r \propto r$ beyond about 5 pc but that interior to 2 pc the distribution levels off, approaching a constant nonzero value of 3.7×10^6 $M_\odot$. "Dark cluster" refers to a hypothetical object. Note that the predictions of a dark cluster model at the center of the Galaxy do not agree with the observational data. (Adapted from a figure courtesy of Reinhard Genzel and Rainer Schödel. For a discussion of an earlier version of this diagram, see Schödel, et al., *Nature*, *419*, 694, 2002.)

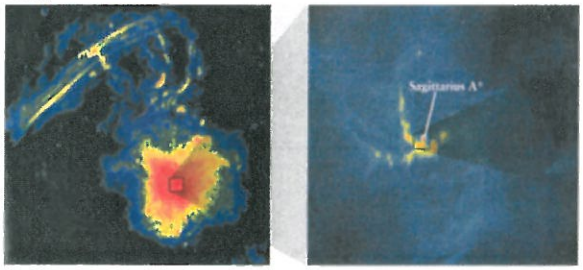

Fig. 24.34 (Left) the central 60 pc × 60 pc of the Galaxy.

Fig. 7. A radio map (λ = 6 cm) of the central 40" of Sgr A West at 0.3" by 0.6" resolution (47), showing the details of the inner bright arms of Sgr A West (Fig. 6). It reveals filamentary structures of very-high-density ($\sim 10^4$ cm^{-3}) ionized gas within the "arms." The white ellipse at the center represents the compact radio source Sgr A*, which has a size of 0.05 arc sec at this wavelength. The filamentary structures and the absence of many unresolved discrete sources in the ionized gas tend to rule out embedded young stars as the primary ionizing sources.

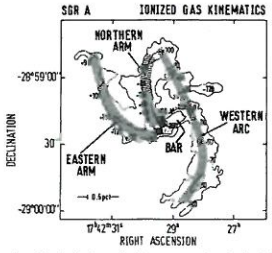

Figure 11 Overview of the ionized gas velocities superposed on the Lo & Claussen (1983) 6-cm map. The measurements in the western arc, bar, and northern and eastern arms are from 12.8-μm [Ne II] spectroscopy by Lacy et al. (1980) and Serabyn & Lacy (1985), and from 76x H 1 recombination-line measurements by van Gorkom et al. (1985, 1987). The $\pm$700 km s^{-1} broad-line emission region is from 2-μm He I/H I spectroscopy by Hall et al. (1982) and Geballe et al. (1984, 1987).

Fig. 24.35 a & b

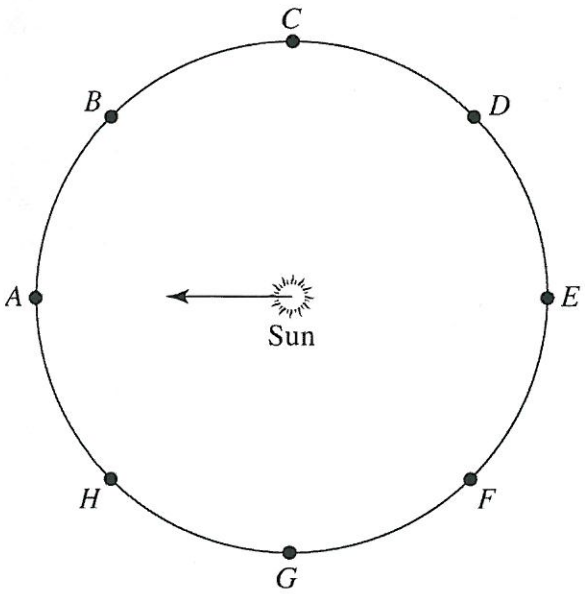

Fig. 24.35 (Prob. 24.36)

p931 High-Energy Emission Lines from Near the GC

511 keV from e-e^+ annihilation $L_{511} \sim 5\times10^4 L_\odot$, but this requires a smaller bh (since smaller bh has higher T_{disk}).
Another source 300 pc from center may be stellar-mass bh which could be source of L_{511}.
Also 1.8-MeV line from decay of $^{26}_{13}Al$, $\tau_{1/2} = 716{,}000$ yr $\Rightarrow$ large # of SNe over past 10^5–10^6 yrs.
"The GC is clearly an extremely dynamic environment.

Ch. 27 - The Structure of the Universe

§27.1 the Extragalactic Distance Scale p1038

It's easy to find the angular coords. R.A. (around celestial equator from vernal equinox, α) + declination (δ degrees N or S), but distances are difficult.
Distances also important because we're looking back in time

Unveiling the 3rd Dimension
Solar neighborhood distances: §3.1.
Trigonometric parallax is now good to several kpc.
We will now describe various methods that are used for different distance ranges: the cosmological distance ladder.

the Wilson-Bappu Effect p.1039
Spectroscopic parallax (§8.2) is a misnomer - it has nothing to do w/ parallax
It is the use of a star's spectrum to determine absolute magnitude $\Rightarrow d(<7\text{ kpc})$
The Wilson-Bappu effect (1956) is the use of the width of the calcium K line to determine the precise spectral type of star.

The Cepheid Distance Scale
There is a relationship, discovered by Henrietta Leavitt (~1908)(§14.1), between period + luminosity of Cepheid variables.
Now we know there is also a small color dependence, modern formula is

$$M_{<V>} = -3.53 \log_{10} P_d - 2.13 + 2.13(B-V)$$ B=blue, V=visual, d=days

1990's Hipparcos (ESA) spacecraft measured parallaxes of 273 Cepheids to ~0.001" to calibrate this.
Overall accuracy goes from 7% for LMC to 15% for more distant galaxies.
Interstellar extinction is the largest source of error.

SNe as Distance Indicators p.1041
If the angular size of a SN photosphere is observed to increase with time this rate, along with $V_{(ejecta)}$ from Doppler, gives d, but most SN too distant for this.
Or use $R(t) = V_{ej}\,t$, get T_e from spectrum, then $L = 4\pi R^2 \sigma T_e^4 \Rightarrow d$.
Uncertainties ~15–25%.